Size-dependent magnetism and spin-glass behavior of amorphous NiO bulk, clusters, and nanocrystals: Experiments and first-principles calculations

J. B. Yi,[1] J. Ding,[1,*] Y. P. Feng,[2] G. W. Peng,[2] G. M. Chow,[1] Y. Kawazoe,[3] B. H. Liu,[1] J. H. Yin,[1] and S. Thongmee[1]
[1]*Department of Materials Science and Engineering, National University of Singapore, Singapore 119260*
[2]*Department of Physics, National University of Singapore, Singapore 119260*
[3]*Institute of Materials Research, Tohoku University, Aoba-ku, Sendai 980-8577, Japan*
(Received 26 July 2007; revised manuscript received 30 September 2007; published 5 December 2007)

A combined experimental and computational study was carried out to investigate magnetic properties of NiO nanostructures. Remarkable size-dependent magnetism was discovered. Uniform amorphous NiO showed a dominated antiferromagnetic interaction and an ordering temperature of 3.5 K. NiO clusters (up to 1 nm) tend to be ferromagnetic interaction with an ordering temperature of 35 K, accompanied by high magnetization (105 emu/g) and a spin-glass behavior. NiO nanocrystals (>2 nm) were found to be antiferromagnetic with uncompensated surface magnetization and shifted hysteresis due to the core-shell interactions.

DOI: 10.1103/PhysRevB.76.224402 PACS number(s): 75.75.+a, 75.50.Ee, 75.50.Lk, 75.70.Rf

Due to important applications in exchange bias and spin-valve devices, nanostructures of antiferromagnetic oxides (also known as nanoclusters, nanocrystallites, or ultrathin layers) have been intensively investigated[1–6] Ferromagnetism with large magnetization was reported in CoO and CuO nanoclusters.[7–10] Uncompensated magnetization with exchange bias and spin-glass behavior was observed in nickel and iron oxides.[11–14] These works have demonstrated that nanostructures of oxides of antiferromagnet have very different properties from the corresponding antiferromagnetic bulk materials.[11–13,15] Despite numerous studies, the intrinsic magnetism of the antiferromagnetic nanostructures has not been very well understood. In particular, magnetic properties of fully amorphous state and structures consisting of very small clusters of antiferromagnetic oxides have not been well studied.[16] Understanding the intrinsic magnetism in nanostructured oxides is not only important for practical applications; it is also of fundamental scientific interests, as it may provide insights to the general relationship of antiferromagnetic oxide nanostructures between structures and properties.

Among the various antiferromagnetic oxides, NiO has attracted much attention because of its relatively high Néel temperature. In this work, we present a systematic study on NiO nanostructures, and through a careful control of the microstructure during sample preparation, we show a remarkable size-dependent evolution of magnetic properties of such nanostructures, covering the entire range from uniform amorphous (a random network of Ni-O bonds), nanoclusters to nanocrystals. Besides the previously reported uncompensated magnetization in nanocrystals,[11,12,17] we found that uniform amorphous NiO had disordered structure with a dominant antiferromagnetic interaction with a very low ordering temperature (similar to Néel temperature) of 3.5 K, and NiO clusters were ferromagnetic with a large magnetization over 100 emu/g and a spin-glass behavior.

NiO nanopowders were prepared by the annealing of the precursors of nickel hydroxide, which was derived from the coprecipitation of Ni_2SO_4 and NaOH solutions. The nickel hydroxide precursors were cleaned with de-ionized water until free of sulfate ions. The cleaned precursors were then rinsed several times with anhydrous ethanol. A large quantity of water could be removed after the washing. The precursors were then centrifuged, followed by an annealing at a temperature between 100 and 900 °C for 1 h in air. Thermal gravitation (TG) examination showed that after the washing process with anhydrous ethanol, the precursor contained about 20 wt % water, indicating the presence of a large amount of nickel hydroxide [$Ni(OH)_2$ corresponds to $NiO \cdot H_2O$ or 19 wt % water]. After drying at 100 °C, TG analysis showed that the residual water was less than 5 wt %. When the powder was annealed at a temperature of 170 °C or higher, there was almost no water according to the TG analysis. The powder was expected to be pure NiO. Therefore, only powders annealed at 170 °C or higher were used in our study. As we could not obtain uniform amorphous NiO from the precipitation method because of the existence of $Ni(OH)_2$ and the necessary drying process higher than 100 °C, sputtering was used for the fabrication of the uniform amorphous NiO sample. The amorphous NiO sample was obtained after the deposition of Ni film under a high oxygen partial pressure on glass substrate at room temperature, similar to that of CoO.[18] X-ray diffraction (XRD) and transmission electron microscopy (TEM) were used in the structural analysis. Magnetic properties were studied with a superconducting quantum interference device (SQUID) system in the temperature range of 2–400 K with a maximum field of 50 kOe. Note that the signal of glass substrate was carefully deducted from the calibration of glass substrate for the amorphous NiO sample.

Figure 1 shows the TEM micrographs of NiO samples. The NiO prepared by sputtering showed a uniform amorphous structure [Fig. 1(a)]. It should be noted that during the TEM examination, the sample was carefully tilted and focused. The NiO samples prepared by precipitation method after the annealing between 100 and 200 °C have a microstructure as shown in Fig. 1(b). We know that there are no clear peaks of crystalline NiO in the XRD study. However, the structure under the high-resolution TEM is not uniform as shown by the nonuniform contrast and some crystalline lattices. The dark field image [Fig. 1(c)] shows that NiO is in a cluster state with a cluster size around 1 nm. Well-

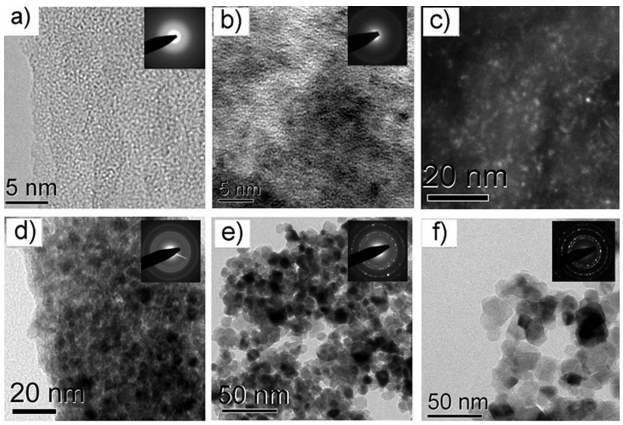

FIG. 1. (a) Bright field TEM micrographs of uniform amorphous NiO sample derived by sputtering. (b) NiO clusters after annealing at 170 °C. (c) The dark field micrograph of NiO cluster after annealing at 170 °C. Bright field TEM micrograph of (d) NiO nanocrystals after annealing at 300 °C. (e) NiO nanocrystals after annealing at 450 °C, and (f) NiO nanocrystals after annealing at 650 °C. The insets show the SAED patterns of the corresponding samples.

crystalline NiO nanocrystals are observed in NiO powders annealed at temperatures higher than 250 °C, and the crystal size increases with the increase in the annealing temperature, as shown in Figs. 1(d)–1(f). The selected area electron diffraction (SAED) patterns in the inset also show the evolution of NiO structures from amorphous to nanocrystalline.

The measured magnetization as a function of the annealing temperature taken at 2 K under the maximum field of 50 kOe is shown in Fig. 2. It can be seen that the uniform amorphous sample (prepared by sputtering) has a very low magnetization. The NiO powder annealed at 100 °C shows a magnetization of 45 emu/g. The magnetization increases with the increase in the annealing temperature and reaches a

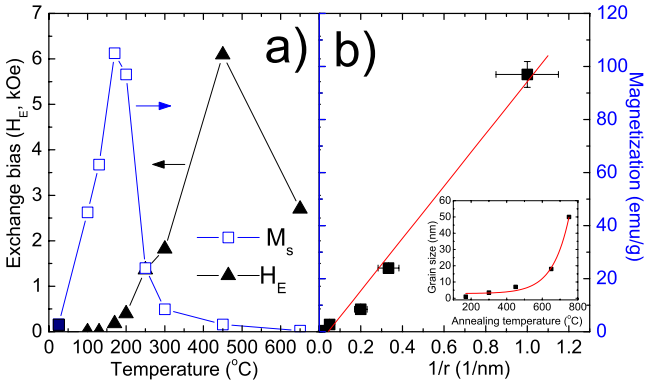

FIG. 2. (Color online) (a) The magnetization (M_s) and exchange bias (H_E) of NiO powders in the dependence on the annealing temperature (M_s was measured under the maximum magnetic field of 50 kOe at the temperature of 2 K). (b) the magnetization versus $1/r$ (r=the radius of the NiO nanocrystal). The magnetization and exchange bias were taken after a field cooling from 400 K under a constant magnetic field of 50 kOe. The inset of (b) is the grain size dependence on the annealing temperature.

maximum of 105 emu/g at the annealing temperature of 170 °C. Annealing at a higher temperature than 170 °C leads to a lower magnetization. The sample annealed at 200 °C possesses a slightly lower magnetization (97 emu/g). Further increasing the annealing temperature results in a drastic decrease of magnetization. For example, NiO powders showed a magnetization of 24 emu/g after annealing at 250 °C and the magnetization reduced to very low values when the annealing temperature was over 450 °C.

Shifted hysteresis loop (exchange bias) has been reported in NiO nanoparticles due to exchange coupling between the antiferromagnetic core and canted magnetic moments on the surface.[11] As shown in Fig. 2(a) a significant exchange bias of 1 kOe is found for the sample after annealing at 250 °C, which is the onset temperature of the appearance of well-crystalline NiO nanocrystals under XRD and TEM. The exchange bias increases with the increase in the annealing temperature, probably due to the enhancement of the exchange coupling and magnetic anisotropy in larger NiO particles. The decrease in exchange bias after annealing at 650 °C is possibly because that the maximum temperature of our SQUID system (400 K) is not sufficient to align the NiO particles. Because of the increase in the total anisotropy energy (with the volume), the alignment might require a field cooling from a temperature above the Néel temperature (around 520 K).[19]

As shown in Fig. 2(a), the measured magnetization at 50 kOe decreases with the increase in the annealing temperature when NiO crystallites are formed (after annealing at 250 °C and higher). From the dark field image of Fig. 1(c), we observe that the crystallite size is approximately 1 nm for the NiO annealed at 170 and 200 °C. We assume that it is in a cluster state. Hence, the curve of the magnetization versus crystallinity size is plotted from the samples annealed at temperatures $\geqslant$200 °C, as shown in Fig. 2(b). It can be seen that the magnetization is inversely proportional to the crystallite size. The result indicates that the magnetization is proportional to the relative surface (surface/volume $=(4\pi r^2)/[(4/3)\pi r^3]\sim 1/r$). The magnetization values of the well-crystalline NiO samples (NiO nanocrystals) support that the magnetization decreasing with the increase in the grain size is attributed to the canted surface magnetization. The inset of Fig. 2(b) indicates the grain size dependence of NiO on the annealing temperature. The grain size increases with the increase in the annealing temperature. A significant increase of grain size could be observed when the annealing temperature was larger than 600 °C.

Canted surface magnetic moment and exchange bias in NiO nanocrystals were reported previously.[11,17,20] Therefore, we pay particular attention to the two samples, namely, the uniform amorphous sample (by sputtering) and the sample with the highest magnetization (after annealing at 170 °C). Our XRD and TEM studies have shown that the sputtering-derived NiO samples possess a uniform amorphous structure. The magnetization curve is shown in Fig. 3(b). No ferromagnetism and/or uncompensated magnetic moment is found. The magnetic susceptibility shows that the average interaction energy is of antiferromagnetic sign. Hence, the film may be a dominant antiferromagnetic interaction with an ordering temperature of 3.5 K, as shown in Fig. 3(a). The paramag-

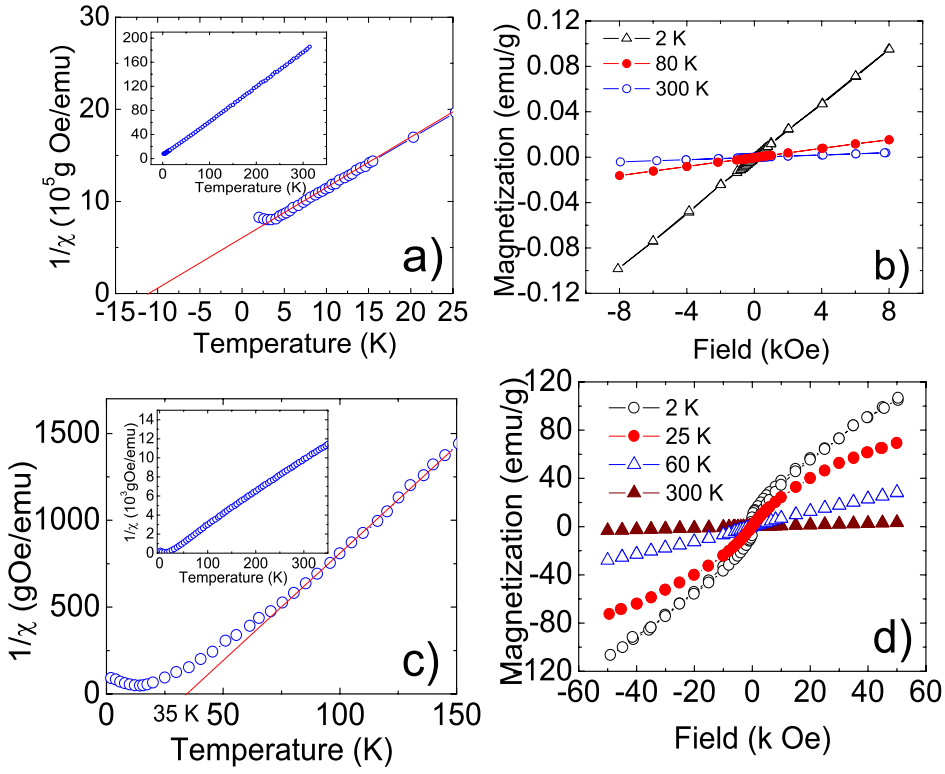

FIG. 3. (Color online) (a) The inverse of susceptibility $1/\chi$ versus temperature for the uniform amorphous sample. The inset shows the inverse of the susceptibility in the whole range of temperature from 2 to 300 K. (b) The magnetization curves of the uniform amorphous sample taken at different temperatures. (c) The reversal of susceptibility versus temperature for the NiO sample annealed at 170 °C. (d) The magnetization curves of the NiO sample annealed at 170 °C.

netic ordering temperature is estimated to be −12 K after the extrapolation of the $1/\chi$ versus temperature curve [based on the magnetic susceptibility $\chi = C/(T-T_c)$]. The relatively large ratio of antiferromagnetic ordering temperature/paramagnetic ordering temperature could be attributed to the structural fluctuation of the amorphous structure.[21]

As shown in Fig. 3(c), the magnetic susceptibility of the sample annealed at 170 °C follows the Curie-Weiss law [$\chi = C/(T-T_c)$], indicating that the powder prefers a ferromagnetic interaction. The ordering temperature is approximately 35 K. The magnetic moment per Ni ion is calculated to be 1.9 μ_B, which is very close to the theoretically expected moment for Ni^{2+} (2 μ_B). Based on the nickel moment of 1.9 μ_B, the calculated saturation magnetization is 142 emu/g. The measured magnetization under the maximum field of 50 kOe was 105 emu/g at 2 K, as shown in Fig. 3(d). The value is approximately 75% of the saturation magnetization, indicating that the sample requires a very high magnetic field to saturate. Since there is no sign of a demagnetization plateau in the susceptibility and the magnetization curves do not show an approach to saturation, it indicates the possibility of an asperomagnetism and/or spin-glass behavior of the powder.[21,22] Zero-field cooling (ZFC) magnetization curves were taken under different magnetic fields for the sample after a postannealing at 170 °C (Fig. 4). At low magnetic fields (<100 Oe), there is a peak of magnetization around 14 K (freezing temperature). The peak shifts to the lower temperature side with the increase in the magnetic field. The cusp temperature under different magnetic fields obeys the relationship $H_{AT}(T)/\Delta J \propto (1-T/T_F)^{3/2}$.[23] The curve of $H^{2/3}$ vs T is shown in the inset of Fig. 4, which is expected for a spin-glass system. No coercivity and remanence are found in the magnetization curves taken in the temperature range of 14–35 K, suggesting superparamagnetism interaction in this

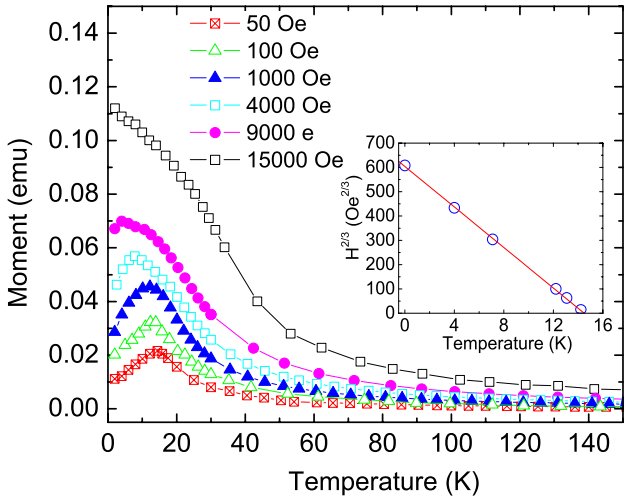

FIG. 4. (Color online) ZFC curves of NiO powders annealed at 170 °C by applying a variety of magnetic fields. The inset shows the curve of the applied field (H) versus the temperature in the cusp (T_P) of the ZFC curves as a function of $H^{2/3}$.

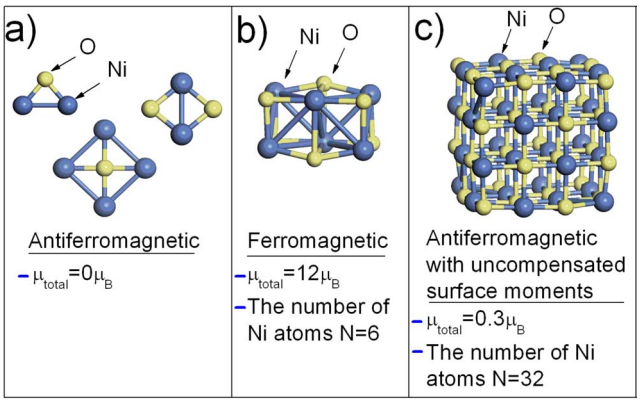

FIG. 5. (Color online) Optimized structures of NiO clusters. (a) Samples with small clusters (Ni_2O, Ni_4O, and Ni_2O_2) showing dominant antiferromagnetic behavior. Spins are compensated through exchange interaction between Ni atoms via oxygen. (b) A sample with medium-sized NiO cluster (Ni_6O_6) favors ferromagnetic behavior. (c) A sample with large antiferromagnetic NiO cluster ($Ni_{32}O_{32}$) showing uncompensated surface moments. Large blue (dark) spheres represent nickel atoms, while small yellow (light) spheres indicate oxygen atoms.

temperature range. Coercivity and remanence are evident in the magnetization curves taken below 14 K, as shown in Fig. 3(d).

In order to understand the evolution of magnetism of NiO (dominant antiferromagnetic coupling in uniform amorphous NiO, ferromagneticlike interaction and spin-glass behavior in NiO nanoclusters, and antiferromagnetic coupling with canted surface moments in well-crystalline NiO nanocrystals), we have performed first-principles calculations to investigate the magnetic properties of NiO clusters as well as their dependence on the cluster size. Using the plane wave method based on the density functional theory, we have studied a series of NiO clusters of various sizes, ranging from a few atoms to several hundred atoms. Details of the calculations, with the projector augmented wave potentials and local spin density approximation and the on site Coulomb interaction, will be reported elsewhere.[24] Our calculation correctly predicts the properties of bulk NiO, which is type II antiferromagnet with spins arranged in alternating ferromagnetically ordered (111) planes. Results of collinear spin polarized calculation show that small and simple cluster structures [in Fig. 5(a)] prefer the antiferromagnetic interaction from the energetic point of view. Due to the simple structures, spin moments from Ni atoms in such small clusters can be easily compensated through exchange interaction between the Ni ions via oxygen. However, for many relatively complicated and medium-sized clusters, especially if all atoms are surface atoms, it becomes difficult for spin compensation. The medium-sized NiO clusters thus favor ferromagnetic state, as demonstrated by one example in Fig. 5(b). When the size of the clusters further increases, the average magnetic moment per Ni decreases rapidly. As shown in Fig. 5(c), the cluster consisting of 32 Ni atoms tends to be antiferromagnetic with a small uncompensated magnetic moment (with a total moment of 0.3 μ_B). Our study on clusters consisting of a total number of Ni atoms from 20 to 100 revealed that the uncompensated magnetic moment is attributed to the Ni atoms on the surface. Uncompensated surface spins are also found in our preliminary noncollinear calculations. Our preliminary calculations for the $Ni_{14}O_{13}$ cluster showed that the optimized noncollinear structure was found to be more stable compared to the collinear one. The total magnetic moment of the most stable noncollinear spin configuration is 1.65 μ_B, which is smaller than that obtained from the collinear spin polarized calculation (2.21 μ_B). Our preliminary work on noncollinear calculations has shown that the collinear calculations can still provide the correct trend for the change of the overall magnetization. However, the preliminary work has shown that noncollinear calculations can provide more accurate results. A detailed and systematic study of noncollinear spin configuration will be carried out in the near future.

The uniform amorphous structure could be understood as a random assembly of simplest Ni-O clusters [as shown in Fig. 5(a)]. Our observation of dominant antiferromagnetic interaction agrees well with our first-principles calculation. Antiferromagnetism is the preferred state of simplest Ni-O clusters which are the elements of the random network of the uniform amorphous structure.

As shown in Fig. 5(b), medium-sized clusters (with 5–10 Ni atoms) tend to be ferromagnetic. The result also agrees qualitatively well with our experimental observations. The $1/\chi$ versus temperature curve obeys the Curie-Weiss law as shown in Fig. 3(c), indicating the dominant ferromagnetic interaction of the clusters in the samples after postannealing at a temperature between 100 and 200 °C. Our experimental results indicate that the ferromagnetism may exist in clusters with a maximum size of approximately 1 nm. The random distribution of magnetic anisotropy of these clusters and/or Ruderman-Kittel-Kasuya-Yosida (RKKY) interactions between clusters may lead to the spin-glass behavior and require a large magnetic field for the magnetization saturation (cluster glass).[21,25] As shown in our first-principles calculations, the ferromagnetic state cannot exist in larger clusters (with a total number of Ni atoms >20). This is because for large clusters, the interior recovers its bulk behavior and therefore remains antiferromagnetic. A weak magnetism is attributed to uncompensated surface moments.

In summary, we have shown a clear scenario of the magnetism of NiO from uniform amorphous, nanocluster to nanocrystals structures. Uniform amorphous NiO shows a disordered structure with a dominant antiferromagnetic coupling, an ordering temperature of 3.5 K, and a paramagnetic ordering temperature of −13 K. NiO clusters with a size of no larger than 1 nm indicate ferromagneticlike interactions, accompanied with a large magnetization over 100 emu/g. The possible presence of the random distribution of magnetic anisotropy of these clusters and/or RKKY interactions between clusters results in a spin-glass behavior. NiO nanocrystals (with a particle size over 2 nm) possess uncompensated magnetization due to the canted surface moments, as shown by exchange bias. Our first-principles calculations also demonstrate that NiO favors ferromagnetic interaction in the nanocluster structure and antiferromagnetic interaction with uncompensated surface magnetization in the well-crystalline structure.

*msedingj@nus.edu.sg

[1] V. Skumryev, S. Stoyanov, Y. Zhang, G. Hadjipanayis, D. Givord, and J. Nogués, Nature (London) **423**, 850 (2003).
[2] Y. H. Wu, K. B. Li, J. J. Qiu, Z. B. Guo, and G. C. Han, Appl. Phys. Lett. **80**, 4413 (2002).
[3] J. Nogués, J. Sort, B. Langlais, V. Skumryev, S. Suriñach, J. S. Muñoz, and M. D. Baró, Phys. Rep. **422**, 65 (2005).
[4] J. Nogués and I. V. Schuller, J. Magn. Magn. Mater. **192**, 203 (1999).
[5] A. E. Berkowitz and K. Takano, J. Magn. Magn. Mater. **200**, 552 (1999).
[6] J. M. Daughton, Thin Solid Films **216**, 162 (1992).
[7] M. Gruyters, Phys. Rev. Lett. **95**, 077204 (2005).
[8] A. Punnoosea and M. S. Seehra, J. Appl. Phys. **91**, 7766 (2002).
[9] M. Gruyters and D. Riegel, Phys. Rev. B **63**, 052401 (2000).
[10] T. Ambrose and C. L. Chien, Phys. Rev. Lett. **76**, 1743 (1996).
[11] R. H. Kodama, S. A. Makhlouf, and A. E. Berkowitz, Phys. Rev. Lett. **79**, 1393 (1997).
[12] S. D. Tiwari and K. P. Rajeev, Thin Solid Films **505**, 113 (2006).
[13] D. T. Margulies, F. T. Parker, F. E. Spada, R. S. Goldman, J. Li, R. Sinclair, and A. E. Berkowitz, Phys. Rev. B **53**, 9175 (1996).
[14] S. D. Tiwari and K. P. Rajeev, Phys. Rev. B **72**, 104433 (2005).
[15] R. H. Kodama, A. E. Berkowitz, E. J. McNiff, Jr., and S. Foner, Phys. Rev. Lett. **77**, 394 (1996).
[16] T. Kaneyoshi, *Introduction to Amorphous Magnetism* (Word Scientific, Singapore, 1992).
[17] R. H. Kodama, J. Magn. Magn. Mater. **200**, 359 (1999).
[18] J. B. Yi and J. Ding, J. Magn. Magn. Mater. **303**, e160 (2006).
[19] W. Meiklejohn and C. P. Bean, Phys. Rev. **102**, 1413 (1956).
[20] S. A. Makhlouf, F. T. Parker, F. E. Spada, and A. E. Berkowitz, J. Appl. Phys. **81**, 5561 (1997).
[21] K. Moorjani and J. M. D. Coey, *Magnetic Glasses* (Elsevier, Amsterdam, 1984).
[22] L. Wang, J. Ding, A. Roy, J. Ghose, Y. Li, and Y. P. Feng, J. Phys.: Condens. Matter **12**, 9969 (2000).
[23] R. L. de Almeida and D. J. Thouless, J. Phys. A **11**, 983 (1978).
[24] G. W. Peng, Y. P. Feng, J. Ding, and Y. Kawazoe (unsubmitted).
[25] L. Wang, J. Ding, H. Z. Kong, Y. Li, and Y. P. Feng, Phys. Rev. B **64**, 214410 (2001).